First-principles study of low-index surfaces of lead

Dengke Yu and Matthias Scheffler
Theory Department, Fritz-Haber-Institut der Max-Planck-Gesellschaft, Faradayweg 4-6, D-14195, Berlin-Dahlem, Germany
(Received 11 May 2004; published 28 October 2004)

We report a density-functional theory study for Pb(111), Pb(100), and Pb(110) surfaces using *ab initio* pseudopotentials and a plane-wave basis set. Creating the pseudopotential with the 6*s*, 6*p*, and 6*d* states in the valence shell is found to yield good results for the bulk lattice constant, bulk modulus, and cohesive energy. Convergence of the surface energies with plane-wave cutoff, **k**-mesh, vacuum and slab thickness was carefully checked, as was the effect of the nonlinearity of the core-valence exchange-correlation interaction. Employing the local-density approximation of the exchange-correlation functional we obtain excellent agreement of the calculated surface energies and surface-energy anisotropies with recent experimental results. However, with the generalized gradient approximation the calculated surface energies are about 30% too low. For all three studied surfaces, the calculations give interlayer relaxations that are in reasonable agreement with low-energy electron diffraction analysis. The relaxations exhibit a damped oscillatory behavior away from the surface, which is typical for a metal surface.

DOI: 10.1103/PhysRevB.70.155417 PACS number(s): 68.35.Md, 68.35.Bs

I. INTRODUCTION

Surface free energies are important material properties that control the shape of crystals and crystallites as well as their stability, and they also affect the growth and stability of films. Only recently it became possible to experimentally determine the *absolute* surface free energies. Using scanning tunneling microscopy (STM) as function of temperatures (well below the melting point) Bonzel determined the equilibrium crystal shape (ECS) of lead crystallites. Then the temperature dependence of the ECS was analyzed by employing classical lattice models. For the low-index surfaces of lead, the surface energies, step energies, and kink formation energies were obtained as best fit parameters and then extrapolated to zero Kelvin.[1–4] This experimental work forms the basic motivation for our density-functional theory study with the intention to provide an independent check of the employed methodology. Furthermore, this experimental study enables us to analyze the accuracy of state-of-the-art exchange-correlation functionals for the description of surface energies, also providing deeper, microscopic insight into what is behind these important parameters. As a first step, we will study in the present paper the surface energies of Pb(111), Pb(100), and Pb(110).

The experimentally reported surface free energies for Pb(111) is 27.5 ± 1.4 meV/Å^2 at 323 K–393 K, and the temperature dependence was found to be insignificant.[3] Interestingly, the comparison with various existing theoretical results reveals a significant scatter of the latter. Obviously, this is most unsatisfactory, in particular because the origin of the scatter and the noticeable differences to the experimental values is unknown. The different calculations employed different methodologies: the pseudopotential plane-wave (PPW) method[5] and ultrasoft pseudopotential plane-wave (UPPW) method,[6] a full charge density linear muffin-tin-orbitals method in the atomic sphere approximation (FCD LMTO-ASA),[7] and a full-potential Korringa-Kohn-Rostoker (FP KKR) method.[8] Adding to the confusion is that these different methods were used together with different approximations of the exchange-correlation functional: the local-density approximation (LDA) as parametrized by Perdew and Zunger (LDA-PZ)[9], the LDA as parametrized by Vosko, Wilk, and Nusair (LDA-VWN),[10] the generalized gradient approximation (GGA) of Perdew and Wang (GGA-PW91),[11] and the (very similar) GGA of Perdew, Becke, and Ernzerhof (GGA-PBE).[12] All these results are summarized in Fig. 1 together with the experimental value. In this paper we will discuss the influence of various approximations on the theoretical results: influence of the exchange-correlation functional and of the pseudopotential approximation, thickness of the employed slab and vacuum, density of the **k** mesh and the size of plane-wave basis set.

Connected with a calculation of surface energies is the evaluation of the surface relaxation: For the low-index Pb surfaces we find (see Sec. III B) that surface relaxations lower the surface energies of the bulk-truncated geometry by 6% to 16%, depending on the surfaces and exchange-correlation functionals. These changes of surface energy due to relaxations are indeed significant, although they were regarded as small and neglected in previous studies.[7,8]

Experimentally it was found that relaxations of Pb low-index surfaces are quite large compared with other metals.[13–17] Damped oscillatory relaxations were observed in all three Pb surfaces. There are a few models that can account for the damped oscillatory relaxations. The point-ion model of Finnis and Heine,[18] and its modifications,[19] describe a metal as lattice of positive point ions embedded in a uniform background electron charge density. The asymmetry of the electron density at the surface will cause the first layer ions to move inward due to the electrostatic force. As a consequence, deeper layers will move as well. Along this line of thought, Landman, Hill, and Mostoller calculated the electrostatic force acted on each atomic layer, using certain electron density models like a simple step function, the Lang-Kohn density from jellium, etc.[20] In recent first-principles studies it

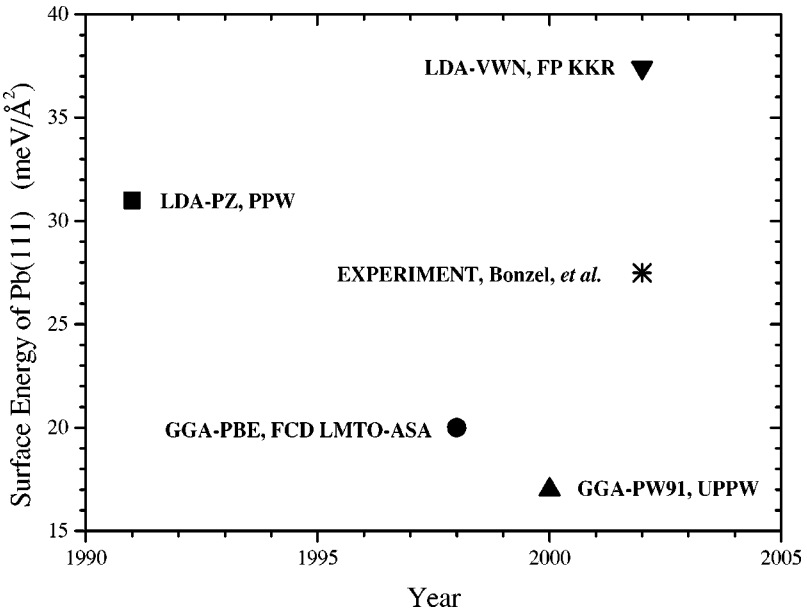

FIG. 1. Various theoretical results of Pb(111) surface energies, compared with experimental values. The exchange-correlation functional and the theoretical method (see text) are shown for each result.

was shown that the Friedel oscillations in electron density near the surface contribute to drive the ions to relax in an oscillatory fashion.[21] On the other hand, Allan and Lannoo related the damped oscillations to a phonon dispersion with complex wave number.[22] In this paper we present first-principles results of the relaxations of all three surfaces. We find reasonable agreement with experimental values. DFT calculations of surface relaxations were so far published only for Pb(111),[6] and the agreement with the experimentally determined values was mediocre. The reason for the difference of theoretical results will be discussed below.

Our DFT calculations of the surface energies and surface relaxations of Pb(111), Pb(100), and Pb(110) were carried out with the FHI98MD package, which employs norm-conserving pseudopotentials and a plane-wave basis set.[23] Both LDA-PZ and GGA-PBE exchange-correlation functionals were used. For the LDA we find that the obtained surface energies and their anisotropy ratios are in excellent agreement with recent experimental results.[3] However, the GGA gives surface energies that are about 30% too low, where the anisotropy ratios are also in good agreement with experimental results (and with the LDA results). The calculated surface relaxations from LDA and GGA are very similar, and are in good agreement with low-energy electron diffraction (LEED) analysis.[14–17]

The remainder of the paper is organized as follows. In Sec. II we summarize our detailed tests of the various numerical and technical approximations employed. In Sec. III we then discuss our final results of surface energies and relaxations, also comparing our findings with previous theoretical results and with the experimentally determined values. Finally, Sec. IV summarizes this work and gives an outlook towards future studies.

II. TECHNICAL TESTS

Motivated and puzzled by the apparent uncertainty of previous theoretical results and the unclear reason for the origin of the scatter of the calculated surface energies (cf. Fig. 1), we performed detailed tests of the various numerical and technical parameters of DFT total energy calculations. This concerns the quality of the pseudopotential (e.g., for describing the bulk properties), and the convergence of surface energies with the plane-wave basis set, **k**-mesh, slab thickness, and vacuum thickness.

A. Pseudopotentials and bulk properties

We use the Hamann-type norm-conserving pseudopotentials[24] in the fully separable Kleinman-Bylander form,[25] generated by the FHI98PP package.[26] Relativity is considered at the scalar relativistic level.[26] Spin-orbital coupling is typically believed to be unimportant for calculated total energies and structures. For Pb Christensen *et al.*[27] had shown that it changes the total energies of a given structure by only $\leqslant 0.05$ eV per atom (see also Ref. 28). Therefore, spin-orbital coupling is not considered in our study of total energies and forces. The 6*s*, 6*p*, and 6*d* orbitals are chosen as valence states, using cutoff radii R_c of 1.27 bohr (6*s*), 1.57 bohr (6*p*), and 1.80 bohr (6*d*). The reference eigenenergy is chosen as +13.50 eV for 6*d*. The cutoff radius and eigenenergy of the unbound 6*d* state are chosen such that the 6*d* pseudopotential approaches the Coulomb potential at distance larger than half the bond length ($\sim$3 bohr). This yields reasonable lattice constant of Pb. To correct for the nonlinearity of the core-valence exchange-correlation potential (nonlinear core correction, NLCC), the core electron density between 0 and 2.20 bohr is treated in the "partial core approximation."[29] The cutoff radius 2.20 bohr is the position where core charge density equals valence charge density. It is somewhat large, but we carefully checked for bulk properties that our treatment gives an accurate description: Also smaller radii for the "partial core density" give the same results for a_0, B_0, and B_0'. The noted setup was used to generate pseudopotentials for both the LDA and the GGA. Transferability was tested by inspecting the pseudoatom wave functions,

TABLE I. Comparison of various properties of Pb bulk. cohesive energy (E^{coh}), lattice constant (a_0), bulk modulus (B_0), and pressure derivative of bulk modulus (B_0') are shown. PPW labels results obtained with the norm-conserving pseudopotential plane-wave method; UPPW refers to ultrasoft pseudopotential plane-wave calculations; FP-APW+lo stands for all electron full potential augmented plane wave plus local orbitals method; 5*d* indicates that Pb 5*d* orbitals are treated as valence orbitals; NLCC labels calculations with the nonlinear core correction applied; SO refers to spin-orbital coupling. The different parametrizations for the local-density approximation (LDA) are noted by W (Wigner), PZ (Perdew-Zunger), and those for the generalized gradient approximation (GGA) are PW91 (Perdew-Wang) and PBE (Perdew, Becke, Ernzerhof).

Method	E^{coh} (eV)	a_0 (bohr)	B_0 (GPa)	B_0'
PPW, LDA-PZ	3.83	9.16	52.6	5.2
PPW, LDA-PZ, NLCC	3.67	9.30	50.4	4.9
PPW, LDA-PZ, 5*d*	3.76	9.25	50.6	5.0
PPW, GGA-PBE	2.99	9.56	39.3	4.7
PPW, GGA-PBE, NLCC	2.87	9.60	38.6	4.5
PPW, LDA-W, NLCC, SO[a]		9.33	46.2	4.6
PPW, LDA-PZ, NLCC[b]		9.24	53	
UPPW, GGA-PW91[c]		9.54		
FP-APW+lo, LDA-PZ[d]	3.7	9.23	52.5	5.0
FP-APW+lo, GGA-PBE[d]	2.9	9.52	39.5	4.7
Experiment[e]	2.02	9.35	43.2	4.9

[a]Reference 28.
[b]Reference 5.
[c]Reference 6.
[d]Reference 31.
[e]References 32 and 33.

excitation energies, etc., with the corresponding values of the all-electron atom. Pseudopotentials with 5*d* orbitals as valence orbitals are also generated. For this we used the following R_c values: 0.85 bohr (5*d*), 1.27 bohr (6*s*), and 1.57 bohr (6*p*).

Let us briefly summarize the resulting bulk properties, and for that we use the primitive fcc unit cell, a Monkhorst-Pack mesh[30] of $12\times12\times12$, and a Fermi-smearing temperature of 0.2 eV. This **k** mesh corresponds to 182 points in the irreducible part (1/48) of the first Brillouin zone. Twelve lattice parameters within the range of ±1.0 bohr around the equilibrium lattice constant were used to evaluate total energies and the results were then fitted by the Murnaghan equation of state, in order to obtain the bulk modulus B_0 and its derivative B_0'. By testing different setups, e.g., the number of data points of different lattice parameters, and their range of deviation from the equilibrium lattice constant, we estimate that the numerical error bar for B_0 is ±2 GPa, and for B_0' it is ±0.2. The equilibrium lattice constant is not sensitive to the fitting procedure. To calculate the cohesive energy, we need the energy of the pseudoatom. A simple cubic cell of 50 bohr, the same pseudopotentials and basis sets as in the bulk calculations were used to calculate the total energy of the spin-saturated pseudoatom. The energy decrease due to spin-polarization is obtained from the all-electron calculation with the FHI98PP code. For the LDA this gives 0.48 eV, and for the GGA the value is 0.60 eV. Testing the plane-wave basis set (increasing it up to 40 Ry) we find for both, the LDA and the GGA, that the bulk cohesive energy and the bulk modulus are well converged already at 14 Ry. Compared with the results at $E^{cut}=40$ Ry the cohesive energy and bulk modulus at $E^{cut}=11$ Ry differ by only −78 meV and −1 GPa, respectively. The lattice constant is practically unchanged. For our pseudopotential with the 5*d* states as valence states, a plane-wave basis with $E^{cut}=50$ Ry is required in order to obtain good convergence.

The calculated cohesive energy, lattice constant, and bulk modulus are listed in Table I where these results are also compared with those of other theoretical and experimental studies. It can be seen that for the LDA the inclusion of NLCC gives rise to a decrease of the cohesive energy by 0.16 eV, an increase of the lattice constant by 0.14 bohr, and a decrease of the bulk modulus by 2.2 GPa. On the other hand, for the GGA calculation the lattice constant and bulk modulus change only little when the NLCC is applied, while the cohesive energy decreases by 0.12 eV. All our pseudopotential results with the NLCC are in good agreement with the results of all-electron FP-APW+lo calculations by Blaha.[31] The differences, e.g., 50.4 GPa (for PPW) and 52.5 GPa (for FP-APW+lo), which is the biggest one, are indeed insignificant.

Table I also gives the PPW results for treating the 5*d* states as valence states (line, PPW, LDA-PZ, 5*d*). These calculations, which are much more expensive, as they require a very high energy cutoff for the basis set, give essentially the same result as our "standard" pseudopotential. This finding is indeed not unexpected because the Pb 5*d* band is fully occupied, lies well below the Fermi level (about −17 eV), and has a very narrow bandwidth (about 0.5 eV). Thus 5*d* orbitals do

TABLE II. Tests of the influence of the thickness of vacuum region. Pb(111), $(1\times\sqrt{3})$ supercell with six bulk atomic layers. This unit cell is rectangular and is twice as large as the (1×1) primitive cell; Pb(100) and Pb(110), (1×1) unit cell of nine bulk atomic layers. 11 Ry plane-wave cutoff, NLCC included. The Monkhorst-Pack **k** mesh used for (111) is 18×10, for (100) is 18×18, for (110) is 18×12. The electronic temperature used for the **k** integration is 0.2 eV. Surfaces are not relaxed. XC refers to the type of exchange-correlation functional. Surface energies γ are given in meV/Å^2, and work functions ϕ are given in eV.

	Vacuum	20 bohr		24 bohr		28 bohr		32 bohr	
XC	Face	γ	ϕ	γ	ϕ	γ	ϕ	γ	ϕ
LDA	(111)	26.86	*4.07*	26.80	*4.07*	26.71	*4.08*	26.82	*4.07*
LDA	(100)	31.78	*4.07*	31.78	*4.06*	31.74	*4.07*	31.74	*4.06*
LDA	(110)	34.85	*3.92*	34.77	*3.92*	34.75	*3.93*	34.74	*3.93*
GGA	(111)	17.78	*3.78*	17.81	*3.76*	17.68	*3.77*	17.78	*3.78*
GGA	(100)	22.11	*3.80*	22.14	*3.78*	22.12	*3.75*	21.94	*3.80*
GGA	(110)	24.21	*3.63*	24.27	*3.65*	24.13	*3.65*	24.05	*3.66*

not play an important role in the bonding and it is therefore appropriate to treat them as core states, "hidden" in the pseudopotential.

Compared with experimental results,[32] our LDA+NLCC results for the lattice constant is 0.5% too small, and the bulk modulus is 17% too large. Employing the GGA-PBE functional and also including the NLCC, the lattice constant is 2.7% larger; consequently the bulk modulus is too small (cf. Table I). The cohesive energy is larger than the experimental value,[33] which is a known feature of density-functional theory. We conclude that we have generated good quality pseudopotentials, that for the bulk properties of Pb give results in agreement with those of full-potential calculations.

B. Surface energies and work functions

The large scatter of the so far published Pb surface energies (cf. Fig. 1) also calls for careful tests of the slab approach. Thus, in this subsection we will discuss the dependence of surface energies and work functions on the slab thickness, vacuum thickness, plane-wave cutoff, **k** mesh, and the effect of nonlinearity of the core-valence exchange-correlation interaction.

All previous studies (except for the FCD LMTO calculations), and also this publication, employed the "repeated slab" model to simulate a surface. Thus, the three-dimensional unit cell is periodic in all three dimensions, and the slabs are separated by a vacuum region of finite width. The typically most sensitive quantity of such approach is the slab thickness, i.e., if one likes to describe the surface of a macroscopic crystal, one must ensure that the thickness is sufficiently large so that the through-slab interaction of two surfaces of the slab is negligible. We therefore checked the convergence of surface energies and work functions with slab thickness. For thin slabs we find considerable oscillations of the surface energies and work functions that reflect the existence of quantum size effects (see e.g. Ref. 34 for a jellium study of such effects). Details of the quantum size effects, how they differ for different surface orientations, and how they affect relaxations will be discussed elsewhere. Here we just note that for a slab thickness larger than six lattice constants ($\sim$60 bohr), the surface energies and work functions are well converged. This corresponds to about 10 layers for the Pb(111) surface, 12 layers for Pb(100), and 17 layers for Pb(110).

Obviously, the thickness of the vacuum must be sufficiently large so that the through-vacuum coupling between neighboring slabs is negligible, though this is an easy to fulfill condition. For this analysis we used unrelaxed slabs, and the results for Pb(111), Pb(100), and Pb(110) are given in Table II. For a vacuum thickness of 20 bohr the surface energy is found to be converged within 0.2 meV/Å^2 in both LDA and GGA. And the work function is converged for this thickness within 0.02 eV in LDA, and 0.05 eV in GGA.

Table III summarizes our tests of the plane-wave basis set. For $E^{\mathrm{cut}}=14$ Ry, the surface energies are converged within 0.1 meV/Å^2, and the work functions within 0.02 eV. For a

TABLE III. Tests of the plane-wave basis set. Same as in Table II, except that vacuum thickness is set to 20 bohr.

	E^{cut}	11 Ry		14 Ry		16 Ry		20 Ry	
XC	Face	γ	ϕ	γ	ϕ	γ	ϕ	γ	ϕ
LDA	(111)	26.86	*4.07*	27.04	*4.09*	27.02	*4.08*	27.11	*4.09*
LDA	(100)	31.78	*4.07*	32.06	*4.07*	32.00	*4.07*	32.12	*4.07*
LDA	(110)	34.85	*3.92*	35.13	*3.92*	35.09	*3.92*	35.21	*3.93*
GGA	(111)	17.78	*3.78*	18.41	*3.78*	18.40	*3.78*	18.47	*3.78*
GGA	(100)	22.11	*3.83*	22.67	*3.79*	22.68	*3.77*	22.72	*3.77*
GGA	(110)	24.21	*3.63*	24.87	*3.63*	24.92	*3.64*	24.98	*3.64*

TABLE IV. Tests of the accuracy of the **k** integration using different Monkhorst-Pack mesh. Same as in Table II, except that the vacuum thickness is 20 bohr. **k** mesh 24 stands for 24×14, 24×24, and 24×17 for Pb(111), Pb(100), and Pb(110). In **k** mesh 36 the density is twice that of 18 in both directions of each slab (see Table II). Only one **k** point is used in direction perpendicular to the surface.

k mesh		18		24		36	
XC	Face	γ	ϕ	γ	ϕ	γ	ϕ
LDA	(111)	26.86	*4.07*	27.04	*4.09*	27.02	*4.08*
LDA	(100)	31.78	*4.07*	32.06	*4.07*	32.00	*4.07*
LDA	(110)	34.85	*3.92*	35.13	*3.92*	35.09	*3.92*
GGA	(111)	17.78	*3.78*	18.41	*3.78*	18.40	*3.78*
GGA	(100)	22.11	*3.83*	22.67	*3.79*	22.68	*3.77*
GGA	(110)	24.21	*3.63*	24.87	*3.63*	24.92	*3.64*

metal also the **k** mesh used for the Brillouin zone integration must be tested carefully. Table IV lists some of our results for the surface energies and work functions in dependence on the Monkhorst-Pack **k** mesh. Within both LDA and GGA, the **k** meshes of 24×24 for Pb(111) and Pb(100), and 24×17 for Pb(110) have converged the surface energies to 0.05 meV/Å^2, and work functions to 0.02 eV. They correspond to 156 **k** points for Pb(111) unit cell, 78 points for Pb(100) unit cell, and 108 points for Pb(110) unit cell. In practice, we used a rectangular supercell of $(1\times\sqrt{3})$ for Pb(111) in our calculations, which is twice as large as the (1×1) unit cell (see Table II).

We also checked the influence of the nonlinearity of the core-valence exchange correlation interaction on the surface energies, as well as the influence of the 5*d* states by using them as valence states. The results are listed in Table V. The surface energies with NLCC decrease by about 2 meV/Å^2 in both LDA and GGA. Compared with the GGA surface energies of ~20 meV/Å^2, it is advisable to include the NLCC. When treating 5*d* as valence states, the surface energies decrease by a smaller amount of about 1 meV/Å^2. This may be due to the fact that including the 5*d* states in the self-consistent cycle, the frozen-core approximation is partially lifted. However, as the changes in surface energies are small, and the computational cost is tremendous (the required plane-wave basis set cutoff is 50 Ry), we will use the pseudopotential that incorporated the 5*d* states in the core.

In summary, for converged high quality pseudopotential calculations we consider it necessary to use a vacuum thickness of 20 bohr, slabs of thickness larger than six lattice constants (~60 bohr), a plane wave cutoff of 14 Ry, Monkhorst-Pack **k** meshes of 24×24 for Pb(111) and Pb(100), 24×17 for Pb(110), and to include the NLCC.

III. DISCUSSIONS ON SURFACE ENERGIES AND SURFACE RELAXATIONS

A. Surface energies

The surface energies, as calculated with the above described technical setup, are given in Table VI, where they are compared with theoretical results of previous studies as well as to the experimentally obtained values. This shows that differences between different theoretical studies are due to the specific exchange-correlation functional, the inclusion or neglect of surface relaxation, the inclusion or neglect of the NLCC, and to the accuracy of different methods.

First of all, we note that our surface energies obtained within the GGA agree with those of the other three GGA calculations within ±10%. Our LDA surface energies also agree with previous LDA results within ±10%.[5,35] There is a general trend that the GGA results are about 30% lower than the LDA results. The especially high surface energies calculated with the FP-KKR approach and the LDA-VWN functional,[8] is probably largely due to difficulties of the KKR

TABLE V. Tests on the influence of nonlinear core correction and the affect of Pb 5*d* bands. Same as in Table II, but with a vacuum thickness of 20 bohr. Both unrelaxed and relaxed surface energies are shown. *U* denotes an unrelaxed surface, and *R* denotes a relaxed surface. 5*d* means that Pb 5*d* orbitals are treated as valence orbitals, with a plane-wave cutoff of 50 Ry.

Face		(111)		(100)		(110)	
XC	Core effect	$\gamma(U)$	$\gamma(R)$	$\gamma(U)$	$\gamma(R)$	$\gamma(U)$	$\gamma(R)$
LDA		28.52	27.30	33.56	31.87	36.74	31.75
LDA	NLCC	26.86	25.43	31.78	29.97	34.85	30.07
LDA	5*d*	27.37		32.86		35.95	
GGA		19.68	18.39	24.01	22.16	26.41	22.36
GGA	NLCC	17.78	16.30	22.11	19.98	24.21	20.07

TABLE VI. Final results of surface energies, and comparison with other results. *U* and *R* are unrelaxed and relaxed results, 5*d* indicates that 5*d* orbitals are treated as valence orbitals. The surface energies of Pb(111), Pb(100), and Pb(110) surfaces within LDA and GGA are calculated from slabs of 12, 14, and 18 layers. The vacuum thickness is 20 bohr, plane-wave cutoff is 14 Ry, the **k** mesh is mesh 24 in Table IV. The bulk total energies are calculated from bulk unit cells formed by (111), (100), and (110) layers, with **k** mesh consistent with those used in the slab calculations, which implies an optimum error cancellation.

Method	$\gamma(111)$ (meV/Å^2)	$\gamma(100)$ (meV/Å^2)	$\gamma(110)$ (meV/Å^2)
PPW, LDA-PZ, NLCC, *U*	27.5	32.0	35.0
PPW, LDA-PZ, NLCC, *R*	26.0	29.9	30.8
PPW, GGA-PBE, NLCC, *U*	18.8	22.5	24.7
PPW, GGA-PBE, NLCC, *R*	17.2	20.0	20.8
UPPW, GGA-PW91, *R*[a]	17		
UPPW, GGA-PW91, 5*d*, *R*[b]	16.4		
FCD LMTO-ASA, GGA-PBE, 5*d*, *U*[c]	20.0	23.5	27.8
PPW, LDA-PZ, NLCC, *U*[d]	31		37
UPPW, LDA-PZ, 5*d*, *R*[b]	24.2		
FP KKR, LDA-VWN, 5*d*, *U*[d]	37.4	40.0	44.9
Experiment at 323 K[e]	27.5	29.2	30.1

[a]Reference 6.
[b]Reference 35.
[c]Reference 7.
[d]Reference 8.
[e]Reference 3.

approach in handling the inhomogeneity of electron density at the surface. Also the VWN may play a role, but from other studies we believe that the differences between VWN and other LDA functionals are not very large. Surface relaxation decreases the surface energies by 1.5 to 4.2 meV/Å^2 in the LDA, and 1.6 to 3.9 meV/Å^2 in the GGA. Thus, within the LDA the surface energies decrease by 5.5%, 6.6%, and 12.0% for Pb(111), Pb(100), and Pb(110), and for the GGA the corresponding values are 8.5%, 11.1%, and 15.8%. The effect of surface relaxation to surface energy is therefore significant. For the relaxed surfaces our surface-energy anisotropies are $\gamma(100)/\gamma 111 = 1.16$ and $\gamma(110)/\gamma(111) = 1.21$ (for the GGA-PBE), and $\gamma(100)/\gamma(111) = 1.15$ and $\gamma(110)/\gamma(111) = 1.18$ (for the LDA-PZ). Both, the LDA and the GGA give anisotropy ratios close to the experimental result extrapolated to zero temperature:[3] $\gamma(110)/\gamma(111) = 1.18$.

In simple terms, the surface energy ratio reflects the reduced coordination of the surface atoms with respect to an atom in the bulk (i.e., the number of broken bonds).[36] For the fcc (111), (100), and (110) surfaces the numbers of broken bonds are three, four, and six per surface atom. The number of broken bonds per unit area for the three surfaces are 1, 1.15, and 1.22. Thus in this simple picture the surface energies of the three fcc surfaces should also follow these ratios. Using the surface energies of bulk truncated structures, we get $\gamma(100)/\gamma(111) = 1.16$ and $\gamma(110)/\gamma(111) = 1.27$ for the LDA-PZ, and $\gamma(100)/\gamma(111) = 1.20$ and $\gamma(110)/\gamma(111) = 1.31$ for the GGA-PBE. Thus the broken bond rule is qualitatively applicable, but the differences are noteworthy, in particular for the (110) surface.

Table VI shows that the surface energies obtained with the LDA-PZ functional are in good agreement with the experimental results at 323 K. No clear temperature dependence of $\gamma(111)$ was found in experiment.[3] We can assume that $\gamma(111)$ is very close to its 0 K value at 323 K. Considering the anisotropy ratio of $\gamma(110)/\gamma(111) \sim 1.1$ at 323 K, and ~ 1.18 at 0 K, we expect the change of surface energy is only a few percent at 0 K. Therefore, our calculated surface energies with LDA-PZ functional are in agreement with experimental values to within 10%, which is quite satisfactory. On the other hand, our surface energies obtained with the GGA-PBE functional are noticeably lower (about 30% lower than the experimental values). That LDA gives better surface energies than GGA, is consistent with results from calculations for jellium surfaces. In one of such studies, it was shown that the LDA induced error is small.[37] In a systematic comparison of various exchange-correlation functionals,[38–40] it was found that LDA significantly overestimates the surface exchange energy, while GGA underestimates it (see also Ref. 41). However, due to a better cancellation of errors between surface exchange and correlation energies, LDA gives slightly lower surface exchange-correlation energies than "exact" values, and GGA gives even lower and less accurate values.[39,40]

B. Surface relaxations

Table VII lists the calculated and experimentally determined surface relaxations. Here, in contrast to the above discussed energies, the LDA and the GGA give very much the same description: All three surfaces exhibit a first layer con-

TABLE VII. Comparison of surface relaxations. $\delta d_{i,i+1}$ is defined as the percentage change of layer spacing over that of the bulk value in a certain direction. The technical setups are the same as in Table VI, forces are relaxed to below 5 meV/Å. LEED is the low energy electron diffraction result; IS is the ion scattering result. *A* and *B* label the different structures obtained for Pb(111).

Face	Method	δd_{12} (%)	δd_{23} (%)	δd_{34} (%)	δd_{45} (%)	δd_{56} (%)
(111)	LEED[a]	−3.5±1	0.5±1.4	1.6±1.8		
(111)	LDA (*A*)	−4.4	1.5	−0.1	−0.1	0.1
(111)	LDA (*B*)	−4.6	0.8	−0.3	−0.3	0.0
(111)	GGA (*A*)	−4.8	1.8	−0.3	0.0	0.0
(111)	GGA (*B*)	−5.2	0.9	−0.4	−0.3	0.0
(111)	GGA-PW91[b]	−6.9	0.6	−0.7		
(111)	GGA-PW91[c]	−5.2	2.6	−1.0		
(100)	LEED[d]	−8.0±1.2	3.1±1.2	−3.0±1.2	−2±4	
(100)	LDA	−6.5	2.4	−1.8	0.0	−0.9
(100)	GGA	−7.3	3.1	−2.2	0.4	−0.9
(110)	IS[e]	−17.2±0.5	8.0±2.0			
(110)	LEED[f]	−16.3±1.7	3.4±5.7	−4.0±1.7		
(110)	LDA	−15.7	4.0	−4.2	3.6	−0.1
(110)	GGA	−15.9	3.4	−4.0	3.1	0.4

[a]Reference 17.
[b]Reference 6.
[c]Reference 42.
[d]Reference 16.
[e]Reference 13.
[f]Reference 14.

traction and a second layer expansion. Thus, there is a damped oscillatory relaxation pattern which is in fact the typical behavior found at a metal surface.

For Pb(111), we find that the first layer contraction is slightly larger than the LEED result. The second and third layer relaxations are consistent with the LEED analysis, considering the large error bars. Feibelman got an unusual large first layer relaxation of −6.9% in Pb(111) using a seven-layer slab,[6] and Wei obtained −5.2% for a 12-layer slab.[42] Testing their structures on our 12-layer slab, we find that the energy difference to our optimized structure is rather small [1 to 2 meV per (1×1) cell]. This shows that the potential-energy surface is very flat, and there might be also local energy mimima. This is not a rare situation and we have therefore always used different geometries to start the optimization. We have relaxed them to very small residual forces [below 2 meV/Å for Pb(111)]. Finally we obtained two different structures, named as *A* and *B* (see Table VII). *B* is obtained when starting from Feibelman's structure, and *A* is obtained when starting from the bulk truncated structure and from Wei's structure. With both the LDA and GGA, structure *B* has a larger first layer contraction and a smaller second layer expansion compared to structure *A*. The energies of *A* and *B* are quite close to each other: For the LDA *B* is 0.4 meV lower than structure *A*, for the GGA it is 1.0 meV lower than structure *A*.

For Pb(100), we find that the outer three interlayer spacings are considerably relaxed and in good agreement with experiment. δd_{45} is found to be rather small. For δd_{56} we obtain a −0.9% and for δd_{67} we obtain 0.3%.

For Pb(110), the agreement of our calculations with the LEED results is excellent for the outermost three interlayer spacings. We show that a deeper layer relaxation (δd_{45}) is also considerable, which is almost as large as δd_{23}. Deeper relaxations like δd_{56} and δd_{67} are rather small.

IV. SUMMARY

In summary, the Pb(111), Pb(100), and Pb(110) surfaces were studied by density-functional theory pseudopotential plane-wave calculations. Detailed tests on the technical setup were carried out to identify the possible importance of the various numerical approximations. The generated pseudopotential with Pb 6*s*, 6*p*, and 6*d* as valence orbitals gives a reliable description. Treating the 5*d* orbitals as valence orbitals gives similar accuracy. Then the consideration of the nonlinearity of the core-valence exchange-correlation interaction is found to be necessary.

For the local-density approximation the obtained surface energies and anisotropy ratios are in very good agreement with recent experimental results. For the generalized gradient approximation, however, the absolute surface energies are too small by about 30%. The calculated work functions of the three surfaces with LDA are 0.2 eV to 0.3 eV higher than those with GGA. The calculated surface relaxations with both LDA and GGA are in reasonable agreement with low

energy electron diffraction results. All three surfaces have a noticeable first layer contraction followed by a damped multilayer oscillatory relaxation pattern.

As the next step of our studies, we plan to investigate the step energies, kink energies as well as the step-step interaction energies at Pb(111). This should enable us to compare with corresponding experimental results and to give an independent check of the experimental methodology used to extract the surface energy.

ACKNOWLEDGMENTS

The authors thank Hans P. Bonzel for helpful comments and suggestions, Martin Fuchs for help with the generation of the pseudopotentials, and Peter Kratzer for technical help. The authors are grateful to Peter Blaha for sending us his unpublished results of FP-APW+lo calculations for Pb bulk, and to C. M. Wei and M. Y. Chou for sending us their unpublished relaxation data for Pb(111).

[1] H. P. Bonzel and A. Emundts, Phys. Rev. Lett. **84**, 5804 (2000).
[2] H. P. Bonzel, Prog. Surf. Sci. **67**, 45 (2001).
[3] C. Bombis, A. Emundts, M. Nowicki, and H. P. Bonzel, Surf. Sci. **511**, 83 (2002).
[4] M. Nowicki, C. Bombis, A. Emundts, and H. P. Bonzel, Phys. Rev. B **67**, 075405 (2003).
[5] M. Mansfield and R. J. Needs, Phys. Rev. B **43**, 8829 (1991).
[6] P. J. Feibelman, Phys. Rev. B **62**, 17 020 (2000); **65**, 129902(E) (2002).
[7] L. Vitos, A. V. Ruban, H. L. Skriver, and J. Kollár, Surf. Sci. **411**, 186 (1998).
[8] I. Galanakis, N. Papanikolaou, and P. H. Dederichs, Surf. Sci. **511**, 1 (2002).
[9] D. M. Ceperley and B. J. Alder, Phys. Rev. Lett. **45**, 566 (1980); J. P. Perdew and A. Zunger, Phys. Rev. B **23**, 5048 (1981).
[10] S. H. Vosko, L. Wilk, and N. Nusair, Can. J. Phys. **58**, 1200 (1980).
[11] J. P. Perdew, in *Electronic Structure of Solids '91*, edited by P. Ziesche and H. Eschrig (Akademie Verlag, Berlin, 1991).
[12] J. P. Perdew, K. Burke, and M. Ernzerhof, Phys. Rev. Lett. **77**, 3865 (1996).
[13] J. W. M. Frenken, F. Huussen, and J. F. van der Veen, Phys. Rev. Lett. **58**, 401 (1987).
[14] Y. S. Li, J. Quinn, F. Jona, and P. M. Marcus, Phys. Rev. B **40**, 8239 (1989).
[15] U. Breuer, K. C. Prince, H. P. Bonzel, W. Oed, K. Heinz, G. Schmidt, and K. Müller, Surf. Sci. **239**, L493 (1990).
[16] R. F. Lin, Y. S. Li, F. Jona, and P. M. Marcus, Phys. Rev. B **42**, 1150 (1990).
[17] Y. S. Li, F. Jona, and P. M. Marcus, Phys. Rev. B **43**, 6337 (1991).
[18] M. W. Finnis and V. Heine, J. Phys. F: Met. Phys. **4**, L37 (1974).
[19] P. Jiang, P. M. Marcus, and F. Jona, Solid State Commun. **59**, 275 (1986).
[20] U. Landman, R. N. Hill, and M. Mostoller, Phys. Rev. B **21**, 448 (1980).
[21] J. H. Cho, Ismail, Z. Y. Zhang, and E. W. Plummer, Phys. Rev. B **59**, 1677 (1999).
[22] G. Allan and M. Lannoo, Phys. Rev. B **37**, 2678 (1988).
[23] M. Bockstedte, A. Kley, J. Neugebauer, and M. Scheffler, Comput. Phys. Commun. **107**, 187 (1997).
[24] D. R. Hamann, M. Schlüter, and C. Chiang, Phys. Rev. Lett. **43**, 1494 (1979).
[25] L. Kleinman and D. M. Bylander, Phys. Rev. Lett. **48**, 1425 (1982).
[26] M. Fuchs and M. Scheffler, Comput. Phys. Commun. **119**, 67 (1999).
[27] N. E. Christensen, S. Satpathy, and Z. Pawlowska, Phys. Rev. B **34**, 5977 (1986).
[28] A. Y. Liu, A. García, M. L. Cohen, B. K. Godwal, and R. Jeanloz, Phys. Rev. B **43**, 1795 (1991).
[29] S. G. Louie, S. Froyen, and M. L. Cohen, Phys. Rev. B **26**, 1738 (1982).
[30] H. J. Monkhorst and J. D. Pack, Phys. Rev. B **13**, 5188 (1976).
[31] P. Blaha (private communication).
[32] Y. K. Vohra and A. L. Ruoff, Phys. Rev. B **42**, 8651 (1990).
[33] http://www.codata.org/codata/databases/key1.html
[34] F. K. Schulte, Surf. Sci. **55**, 427 (1976).
[35] C. M. Wei and M. Y. Chou, Phys. Rev. B **66**, 233408 (2002).
[36] See, e.g., M. C. Desjonqueres and D. Spanjaard, *Concepts in Surface Physics* (Springer-Verlag, Berlin, 1993).
[37] J. M. Pitarke and A. G. Eguiluz, Phys. Rev. B **57**, 6329 (1998).
[38] J. P. Perdew, J. A. Chevary, S. H. Vosko, K. A. Jackson, M. R. Pederson, D. J. Singh, and C. Fiolhais, Phys. Rev. B **46**, 6671 (1992).
[39] S. Kurth, J. P. Perdew, and P. Blaha, Int. J. Quantum Chem. **75**, 889 (1999).
[40] V. N. Staroverov, G. E. Scuseria, J. Tao, and J. P. Perdew, Phys. Rev. B **69**, 075102 (2004).
[41] L. Vitos, B. Johansson, J. Kollár, and H. L. Skriver, Phys. Rev. B **62**, 10 046 (2000).
[42] C. M. Wei and M. Y. Chou (private communication).